NUMERICAL STUDY OF TRANSIENT THREE-DIMENSIONAL HEAT CONDUCTION PROBLEM WITH A MOVING HEAT SOURCE

by

Ivana B. IVANOVIĆ [a*]***, Aleksandar S. SEDMAK*** [b]***, Marko V. MILOŠ*** [b]***,***
Aleksandar B. ŽIVKOVIĆ [b]***, and Mirjana M. LAZIĆ*** [b]

[a] Innovation Center, Faculty of Mechanical Engineering, University of Belgrade, Belgrade, Serbia
[b] Faculty of Mechanical Engineering, University of Belgrade, Belgrade, Serbia

Original scientific paper
UDC:536.24:519.728.4
DOI: 10.2298/TSCI1101257I

A numerical study of transient three-dimensional heat conduction problem with a moving source is presented. For numerical solution Douglas-Gunn alternating direction implicit method is applied and for the moving heat source flux distribution Gaussian function is used. An influence on numerical solution of input parameters figuring in flux boundary conditions is examined. This include parameters appearing in Gaussian function and heat transfer coefficient from free convection boundaries. Sensitivity of cooling time from 800 to 500 °C with respect to input parameters is also tested.

Key words*: heat conduction, moving heat source, Gaussian distribution, Douglas-Gunn alternating direction implicit method, cooling time* $t_{8/5}$

Introduction

The problem of transient heat conduction in a plate with a moving heat source captivates attention for many years. There is a great number of theoretical, experimental, and numerical results for this problem starting with the Rosenthal's analytic solution from 1935 [1]. In recent times, with development of the state-of-the-art technologies that expand the possibilities in experimental and numerical research, this interest is renewed and intensified. In addition, The American Weld Society (AWS) has recently initiated a series of activities for the development of the standards for Computational Weld Mechanics (CWM) [2] and the problem of transient heat conduction with moving heat source is the foundation for a larger group of heat transfer problems from the welding industry.

In this work the standard numerical solution of transient three-dimensional heat conduction problem with free convection at all boundaries and additional boundary condition at the top surface induced by the moving heat source is presented. As most apparent for initial numerical analysis, the Douglas-Gunn alternating direction implicit (ADI) method is selected since it is absolutely stable and is of second order in space and time [3, 4]. The same approach is already used in Yeh *et al*. [5] where experimental results for gas tungsten arc welding of

* Corresponding author; e-mail: iivanovic@mas.bg.ac.rs

6061 aluminum plates and S400 soft steel plates are compared to numerical results. The main objective of the current study is numerical experiment. However, some numerical-experimental comparisons are performed using results obtained in work of Lazić *et al*. [6], and therefore, the same material properties and input parameters settings are used as in [6].

In all studied examples, the uniform grid spacing is employed, although from obtained results it is clear that non-uniform grid distribution with finer mesh in proximity of the heat source path would bring advantages and is necessary for the future calculations.

Mathematical model

The model is illustrated in fig. 1. It consists of the plate with dimensions $L \times W \times H$. The trajectory of the heat source is placed at the surface $z = 0$, at the half width of the plate, and coincide with x-axis. Position of the heat source is $x_s = v_x t$, where v_x is constant velocity of the source and t is time.

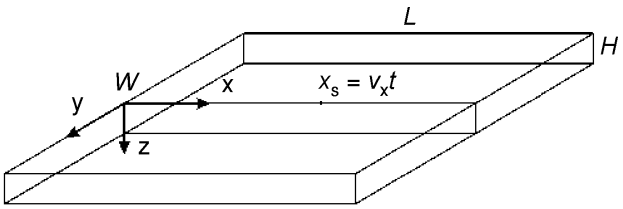

Figure 1. Plate with heat source moving along x-axis

The temperature distribution in the plate is modeled with transient three-dimensional heat conduction equation:

$$\frac{\partial T}{\partial t} = \alpha \left(\frac{\partial^2 T}{\partial x^2} + \frac{\partial^2 T}{\partial y^2} + \frac{\partial^2 T}{\partial z^2} \right) \tag{1}$$

where T is the temperature, $\alpha = k/\rho c_p$ – the thermal diffusivity, k – the thermal conductivity, ρ – the density, and c_p – the specific heat of the material.

Boundary and initial conditions

The main characteristic of this model is a flux boundary condition originating from the heat source which is moving with constant velocity v_x along x-axis at the top surface, $z = 0$. Flux distribution is usually given by the Gaussian function:

$$-k \frac{\partial T}{\partial z} = q_{\max} \exp\left\{ -\frac{c[(x - x_s)^2 + y^2]}{r_0^2} \right\} \qquad z = 0, \quad (x - x_s)^2 + y^2 \le r_0^2 \tag{2}$$

where $q_{\max}$ is the value of the heat flux at the center of the heat source:

$$q_{\max} = \frac{cQ}{r_0^2 \pi}$$

where r_0 is the radius of the heat source, c – the constant, and Q – the power of the heat source.

Free convection with the same value of heat transfer coefficient h is imposed at all other boundary surfaces, including the remaining part of the top surface, and can be presented with following formulas:

$$
\begin{aligned}
k\frac{\partial T}{\partial x} &= h\left(T - T_\infty\right) \qquad x = 0 \\
k\frac{\partial T}{\partial z} &= h\left(T - T_\infty\right) \qquad z = 0, \quad (x - x_\mathrm{s})^2 + y^2 > r_0^2 \\
-k\frac{\partial T}{\partial x} &= h\left(T - T_\infty\right) \qquad x = L \\
-k\frac{\partial T}{\partial y} &= h\left(T - T_\infty\right) \qquad y = \frac{W}{2} \\
-k\frac{\partial T}{\partial z} &= h\left(T - T_\infty\right) \qquad z = H
\end{aligned}
\tag{3}
$$

where T_∞ is the ambient temperature, and h – the heat transfer coefficient.

Since the field is symmetrical with respect to x-axis, half plate is taken into consideration for the calculations and symmetry boundary conditions are imposed at the surface $y = 0$:

$$\frac{\partial T}{\partial y} = 0 \qquad y = 0 \tag{4}$$

All input parameters remain constant during numerical simulation, therefore only position of the heat source, x_s ($t = 0$), and temperature of the plate, T_0, can be taken into account as important initial conditions.

Numerical solution

Douglas-Gunn method is alternating direction method. For the three-dimensional transient heat conduction eq. (1) the method is based on the implicit solutions of *xpts*×*ypts*×*zpts* one-dimensional problems along the grid lines in x, y and z-direction, respectively, where *xpts*, *ypts*, and *zpts* are numbers of grid points in x, y, and z-direction.

Douglas-Gunn three-step ADI method

– for the x-direction:

$$
\begin{aligned}
&-\beta_x T^{n*}_{i-1,j,k} + 2(1+\beta_x)T^{n*}_{i,j,k} - \beta_x T^{n*}_{i+1,j,k} = 2(1-\beta_x-2\beta_y-2\beta_z)T^{n}_{i,j,k} + \\
&+\beta_x(T^{n}_{i-1,j,k} + T^{n}_{i+1,j,k}) + 2\beta_y(T^{n}_{i,j-1,k} + T^{n}_{i,j+1,k}) + 2\beta_z(T^{n}_{i,j,k-1} + T^{n}_{i,j,k+1})
\end{aligned}
\tag{5}
$$

– for the y-direction:

$$
\begin{aligned}
&-\beta_y T^{n**}_{i,j-1,k} + 2(1+\beta_y)T^{n**}_{i,j,k} - \beta_y T^{n**}_{i,j+1,k} = 2(1-\beta_x-\beta_y-2\beta_z)T^{n}_{i,j,k} + \\
&+\beta_x(T^{n}_{i-1,j,k} + T^{n}_{i+1,j,k}) + \beta_y(T^{n}_{i,j-1,k} + T^{n}_{i,j+1,k}) + 2\beta_z(T^{n}_{i,j,k-1} + T^{n}_{i,j,k+1}) + \\
&+\beta_x(T^{n*}_{i-1,j,k} - 2T^{n*}_{i,j,k} + T^{n*}_{i+1,j,k})
\end{aligned}
\tag{6}
$$

– for the z-direction:

$$-\beta_z T_{i,j,k-1}^{n+1} + 2(1+\beta_z)T_{i,j,k}^{n+1} - \beta_z T_{i,j,k+1}^{n+1} = 2(1-\beta_x-\beta_y-\beta_z)T_{i,j,k}^{n} +$$
$$+\beta_x(T_{i-1,j,k}^{n} + T_{i+1,j,k}^{n}) + \beta_y(T_{i,j-1,k}^{n} + T_{i,j+1,k}^{n}) + \beta_z(T_{i,j,k-1}^{n} + T_{i,j,k+1}^{n}) +$$
$$+\beta_x(T_{i-1,j,k}^{n^*} - 2T_{i,j,k}^{n^*} + T_{i+1,j,k}^{n^*}) + \beta_y(T_{i,j-1,k}^{n^{**}} - 2T_{i,j,k}^{n^{**}} + T_{i,j+1,k}^{n^{**}}) \quad (7)$$

for $i = 0, \ldots, xpts\text{-}1$, $j = 0, \ldots, ypts\text{-}1$, and $k = 0, \ldots, zpts\text{-}1$, where $\beta_x = \alpha\Delta t/\Delta x^2$, $\beta_y = \alpha\Delta t/\Delta y^2$, and $\beta_z = \alpha\Delta t/\Delta z^2$, and Δx, Δy, Δz, and Δt are grid spacings and time step.

Discretization of boundary conditions

Numerical formulas for boundary conditions are obtained from boundary condition eqs. (2), (3), and (4) using second order differences in space.

For boundary conditions at surfaces $x = 0$ and $z = 0$

$$T_{-1} = T_1 - C_1 T_0 + C_2 \quad (8)$$

where T_{-1} is the temperature at the imaginary point outside the plate, T_0 and T_1 are temperatures at points i or k equal to zero or one, and coefficients C_1 and C_2 are:

$$C_1 = \frac{2\Delta x h}{k} \qquad C_2 = \frac{2\Delta x h T_\infty}{k} \qquad x = 0$$
$$C_1 = \frac{2\Delta z h}{k} \qquad C_2 = \frac{2\Delta z h T_\infty}{k} \qquad z = 0, \quad (x - x_s)^2 + y^2 > r_0^2$$

and for $z = 0$, $\quad (x - x_s)^2 + y^2 \le r_0^2$

$$C_1 = 0 \qquad C_2 = \frac{2\Delta z}{k} q_{\max} \exp\left\{-\frac{c[(x-x_s)^2 + y^2]}{r_0^2}\right\}$$

For boundary conditions at $x = L$, $y = W/2$, and $z = H$

$$T_n = T_{n-2} - C_1 T_{n-1} + C_2 \quad (9)$$

where n is $xpts$, $ypts$, or $zpts$, and

$$C_1 = \frac{2\Delta x h}{k} \qquad C_2 = \frac{2\Delta x h T_\infty}{k} \qquad x = L$$
$$C_1 = \frac{2\Delta y h}{k} \qquad C_2 = \frac{2\Delta y h T_\infty}{k} \qquad y = \frac{W}{2}$$
$$C_1 = \frac{2\Delta z h}{k} \qquad C_2 = \frac{2\Delta z h T_\infty}{k} \qquad z = H$$

and for symmetry boundary at $y = 0$, $T_{-1} = T_1$.

Results and discussions

A model selected for this numerical study is closely connected to a model presented in the work of Lazić e*t al*. [6]. All simulations are executed for the same material with the

product of density and specific heat, ρc_p = 4898556 J/m^3°C, and the thermal conductivity k = = 36 W/m°C. In addition, the value of the power of the heat source, Q = 4256 W, is retained the same for all numerical simulations. The initial position of the heat source is at x_s (t = 0) = = 6 mm, and the final position is approximately 6 mm from the end of the plate.

Grid vs. moving heat source distribution

For the beginning, a behavior of the numerical solution for different grid distributions is examined. Dimensions of the plate are selected to be L = 250 mm, W/2 = 100 mm, and H = 30 mm, the radius of the heat source, r_0 = 3 mm, and the constant from Gaussian function c = 1. Accordingly to selected dimensions, grid spacings are $\Delta x = \Delta y = \Delta z$ = 0.5, 1, and 2 mm. Initial and ambient temperatures are $T_0 = T_\infty$ = 20 °C, the heat transfer coefficient h = 10 W/m^2°C at all boundaries, the velocity v_x = 1.61 mm/s, and the time step Δt = 0.1 s.

Numerical results for temperature as function of time at the surface z = 4 mm for different grid distributions are illustrated in fig. 2. In the region of an increasing temperature, or in the region where the source is approaching the point, for all presented points, the difference in values of the temperature is less apparent than in the region of decreasing temperature, whereas in the peak temperature region, where the source is in the vicinity of the point, the difference is evident.

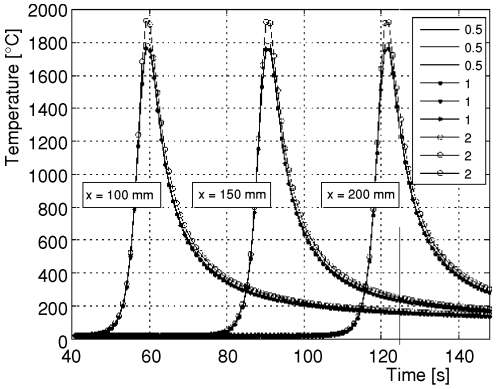

Figure 2. Temperature as function of time at three different position x = 100, 150, and 200 mm, and at the surface z = 4 mm, for three different grid spacings Δx = 0.5, 1, and 2 mm ($\Delta x = \Delta y = \Delta z$)

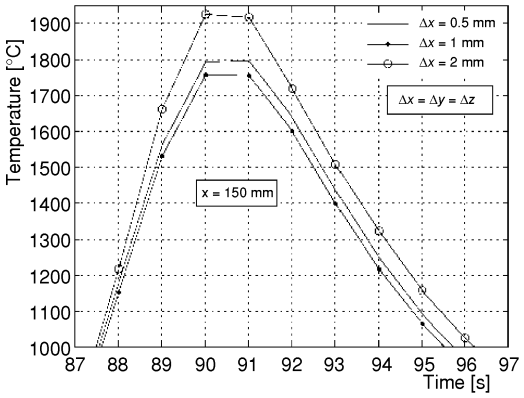

Figure 3. Elements of the fig.2 enlarged

In fig. 3, the region in the vicinity of the peak temperature at the position x = 150 mm is enlarged. It becomes obvious that the solutions for the grid spacings 1 mm and 0.5 mm are in agreement, and that the values of temperature are increasing with the grid refinement. Meanwhile, there is an evident disagreement between these two results and the one obtained with the grid step of $\Delta x = \Delta y = \Delta z$ = = 2 mm. The form of the

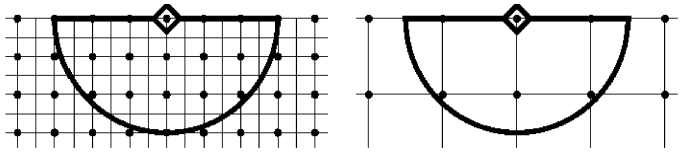

Figure 4. Relation between moving heat source (r_0 = 3 mm) and grid points

current temperature curve follows the form of other two curves but the values of the temperature are remarkably higher.

The relation of the heat source area of radius r_0 = 3 mm and the grid points for different grid spacings enclosed by that area are illustrated in fig. 4. It is evident from this illustration that the difference in the solution for grid spacing of 2 mm is not produced only by the numerical scheme. The number of points enclosed by the area of the source when $\Delta x = \Delta y = 2$ mm is to small for the influence of the heat source to be calculated in the same manner as for the other two grid spacings.

This problem requires detailed analysis since it could have significant influence on the accuracy of the final solution. Certain attempts are already made in refs. [7] and [8] where finite element software Ansys have been used for numerical solution of the similar heat conduction problem.

For other numerical solutions in this study, the grid distribution $\Delta x = \Delta y = \Delta z = 0.5$ mm is chosen combined with the time step $\Delta t = 0.1$ s.

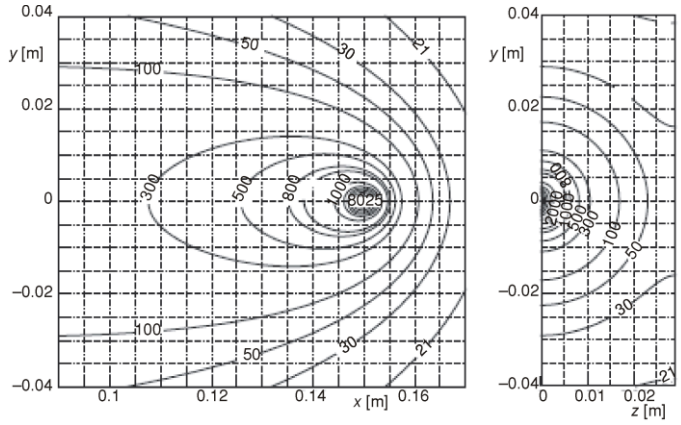

(a) heat source velocity v_x = 1.9 mm/s, surfaces z = 0 and x = 150 mm

(b) heat source velocity v_x = 1.3 mm/s, surfaces z = 0 and x = 150 mm

Figure 5. Temperature distribution for two different heat sorce velocities and for heat source position $x_s \approx 150$ mm at top surface $z = 0$ and at cross-section $x = 150$ mm

Velocity of the moving heat source

The next two examples are selected to test numerical results in the case of two different velocities and to examine the influence of the velocity on the temperature field. A hight of the plat is changed to H = 29 mm, and selected velocities are v_x = 1.3 m/s and v_x = = 1.9 mm/s. The other values are as in the previous example (see subsection *Grid vs. moving heat source distribution*).

The numerical solutions for the heat source position $x_s \approx 150$ mm, at the top surface, $z = 0$ and at the cross-section x = 150 mm, are illustrated at figs. 5. For velocity v_x = 1.3 mm/s source arrive at x_s = 150.04 mm after 1108 time steps or after 110.8 s. For velocity v_x = 1.9 mm/s the exact position is x_s = 150.02 mm after 758 time steps or 75.8 s.

The temperature in the center of the heat source is higher for lower velocity $T \approx 8369$ °C for v_x = 1.3 mm/s, fig. 5(b), compared to $T \approx 8025$ °C for v_x = 1.9 mm/s, fig. 5(a). The contour curves are wider and longer in case of lower velocity, particularly in the regions of lower temperatures in front of the source, which confirm that cooling is slower for lower velocities. In addition, the contour lines are more concentrated in front of the faster source which confirm that, in front of the source, the increase of temperature is faster for the lower velocities [1].

From cross-sections x = 150 mm, illustrated in figs. 5(b) and 5(a), it is obvious that the influence of the slower source is dipper. This is also demonstrated in figs. 6, where temperature as function of time is presented, for several points of the plate, and at surface z = = 7.5 mm. For velocity v_x = 1.3 mm/s, the value of temperature in all points is around 900 °C and higher, fig. 6(b), whereas for velocity v_x = 1.9 mm/s the value of temperature in all points is already considerable under 800 °C, fig. 6(a).

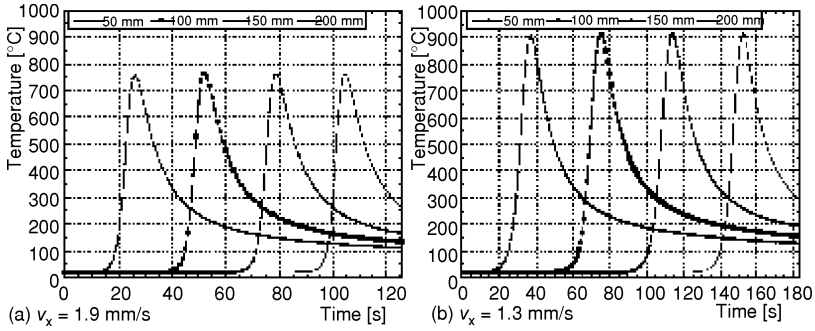

Figure 6. Temperature as function of time at positions x = 50, 100, 150, and 200 mm, and at surface z = 7.5 mm

Cooling time

The next three examples are selected as in Lazić *et al*. [6] to determine the values of the cooling time from 800 to 500 °C from obtained numerical results.

For the first example velocity is v_x = 1.3 mm/s and initial and ambient temperatures are increased to $T_0 = T_\infty$ = 355 °C (see subsection *Velocity of the moving heat source*). The value of the constant in Gaussian function is retained the same, c = 1. Numerical solutions for temperature as function of time at two different surfaces, z = 4 mm and z = 7.5 mm, and for

points at positions x = 50, 100, 150, and 200 mm are illustrated in figs. 7. Temperatures in vicinity of 800 and 500 °C, with corresponding values of time, are marked for first two points. The value of temperature for other points is still above 500 °C at the end of calculation.

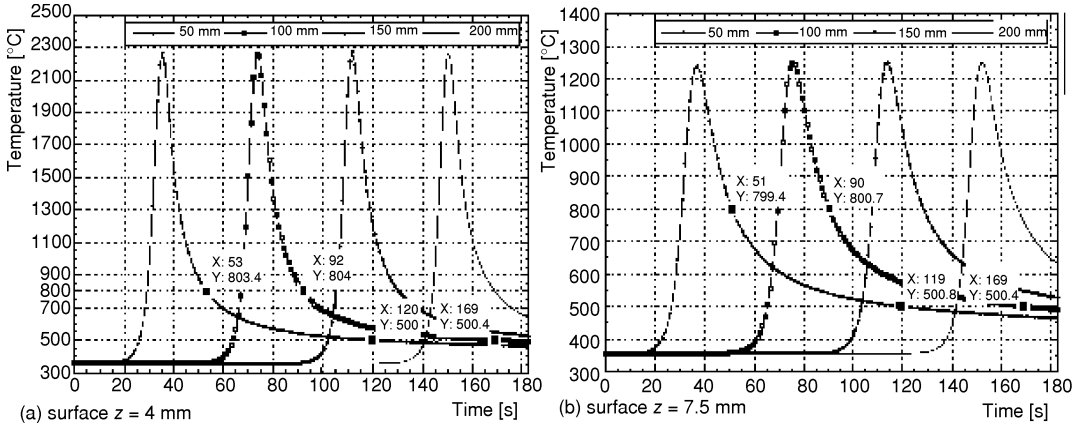

Figure 7. Temperature as function of time at positions x = 50, 100, 150, and 200 mm, for velocity v_x = 1.3 mm/s ($T_0 = T_\infty$ = 355 °C)

The values of cooling time are $t_{8/5}$ = 67 and 68 s for position x = 50 mm, and $t_{8/5}$ = = 77 and 79 s for position x = 100 mm, at surfaces z = 4 mm and z = 7.5 mm, respectively. The cooling of the points at the beginning of the plate is faster, the difference between two positions in x-direction is approximately 10 s. Also the cooling in two depths at the same x position is slightly different, 1-2 s, and it looks like it grows with the depth.

Numerical results for $t_{8/5}$ at position x = 100 mm are in agreement with experimental results obtained in ref. [6].

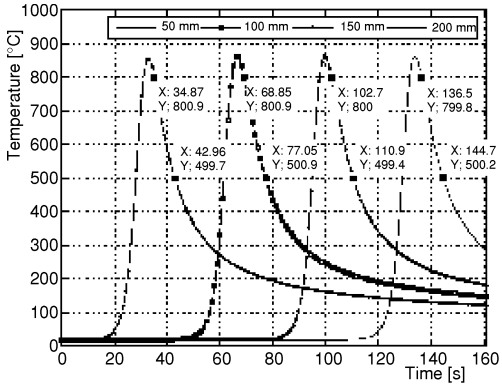

Figure 8. Temperature as function of time at positions x = 50, 100, 150, and 200 mm, and at surface z = 7.5 mm for velocity v_x = 1.48 mm/s ($T_0 = T_\infty$ = 20 °C)

In the second and third example measured values of cooling time obtained from numerical solution are in disagreement with experimental results. For the second example velocity is v_x = 1.48 mm/s and the initial and ambient temperatures are $T_0 = T_\infty$ = 20 °C (fig. 8). The values of cooling time are $t_{8/5}$ = 8.2 s compared to $t_{8/5}$ = 16 s obtained experimentally in ref. [6]. For the third example velocity is v_x = 1.61 mm/s and initial and ambient temperatures are increased to $T_0 = T_\infty$ = 231 °C. The values of cooling time are from $t_{8/5}$ = 16 s to $t_{8/5}$ = 16.9 s compared to $t_{8/5}$ = 25 s obtained experimentally in ref. [6].

Sensitivity to input parameters

An analysis of the influence of input parameters figuring in flux boundary conditions is inspired by the results for the cooling time obtained in the previous subsection. The settings from the second example from the previous subsection are selected as the initial

settings to examine the sensitivity of the final solution to heat transfer coefficient, radius of the heat source, and constant in Gaussian function. The heat source velocity in the current example is v_x = 1.48 mm/s and the temperatures are $T_0 = T_\infty$ = 20 °C.

Solutions for different values of the heat transfer coefficient h and different values of the radius of the heat source r_0 are illustrated in fig. 9. For the heat transfer coefficient two values are tested. The coefficient is reduced from h = 10 to 0.5 W/m^2°C for one calculation and increased to h = 70 W/m^2°C for the other. From fig. 9(a) it is evident that the sensitivity on this parameter is extremely low in the case when the initial temperature of the plate and the ambient temperature are the same. The difference is visible for h = 70 W/m^2°C, mainly in the region of the decreasing temperature, and for temperatures below 500 °C. As expected, the values of temperatures are lower in that region.

For small differences in the dimensions of the radius of the heat source the situation with sensitivity is the same. Two new values of radius are selected, r_0 = 2.5 mm and r_0 = 3.5 mm and the solution is illustrated in fig. 9(b).

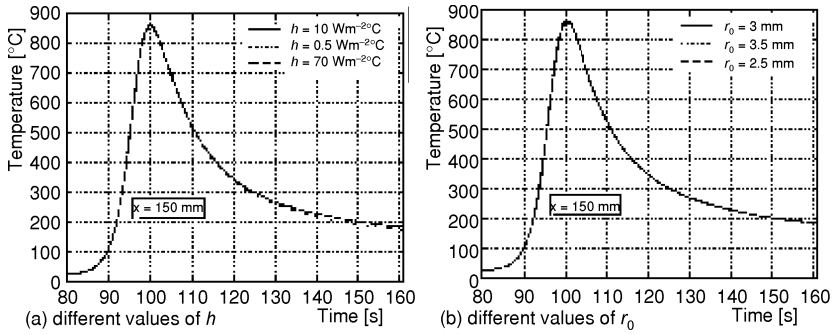

Figure 9. Temperature as function of time at positions x = 150 for velocity v_x = 1.48 mm/s ($T_0 = T_\infty$ = 20 °C)

The important difference in the values of temperature arises in the case of the constant c. In majority of studies this constant is c = 3. In the current study, the value c = 1 is increased to c = 3 to test the sensitivity to this parameter. The results for temperature as function of time are illustrated in fig. 10 compared to the results already presented at fig. 8.

The difference in values of temperature is present in all regions and at all position. The cooling time is increased from $t_{8/5} \approx 8.2$ s to values of $t_{8/5} \approx 10.5$ s to 11.15 s. The values of cooling time are still lower then the one obtained experimentally in Lazić *et al.* [6] but close to the values obtained from empirical formulas given also in ref. [6].

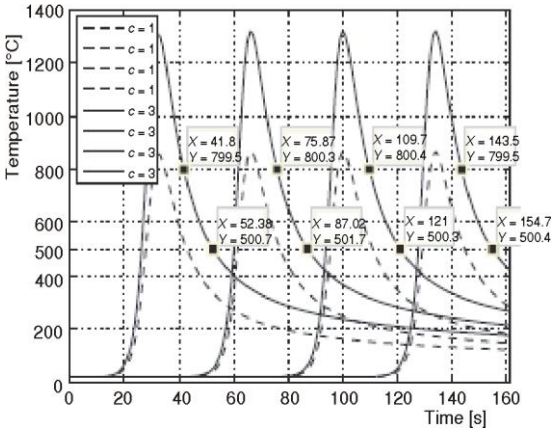

Figure 10. Temperature as function of time at position x = 50, 100, 150, and 200 mm and at surface z = 7.5 mm for velocity v_x = 1.48 mm/s, and for c = 1 and c = 3 ($T_0 = T_\infty$ = 20 °C)

Conclusions

In the current study several numerical experiments have been performed using only one numerical scheme based on finite differences and using the uniform grid distribution. In addition, the Gaussian function has been the only function that is used for heat source flux distribution. It was obvious, from the start, that the behavior of the heat source flux distribution must be further tested. Tests should be performed separately and in conjunction with the velocity of the heat source. This has been partially confirmed in the tests of sensitivity to two parameters: the dimension of the radius of the heat source and the value of the constant from Gaussian function. In numerous studies the values of these two parameters are emphasized as important, and from calculations carried out in this study it looks like the constant has a significant influence on temperature while the radius does not. Certainly, the values of parameters for current calculations have been selected randomly and more profound sensitivity analysis must be performed for further conclusions to be made.

In addition, more attention must be made to the other input parameters. For example, the relation between the initial plate temperature and the ambient temperature, and their influence on the solution is neglected since the equal values have been chosen in all examples. Except the slight change in the thickness in the first example, all dimensions of the plate have been kept the same through the study as well as the value of the power of the heat source. These parameters are important for experimental settings and therefore they are becoming important in numerical study and request more attention in the future.

Acknowledgments

The authors would like to acknowledge the Serbian Ministry of Science and Technological Development for the financial support under Grant TR-14014: Research and development of methods for the estimation of integrity and reliability of welded pipes in petroleum industry.

References

[1] Easterling, K., Introduction to the Physical Metallurgy of Welding, Butterworth–Heinemann Ltd., Oxford, UK, 1992
[2] Babu, S. S., *et al*., How Can Computational Weld Mechanics Help Industry? *Welding Journal, 89* (2010), 1, pp. 40-45
[3] Tannehill, J. C., Anderson, D. A., Pletcher, R. H., Computational Fluid Mechanics and Heat Transfer, Taylor & Francis Ltd., Washington, DC, 1997
[4] Wang, T.-Y., Lee, Y.-M., Chen, C. C.-P., 3-D Thermal-ADI: an Efficient Chip-Level Transient Thermal Simulator, *Proceedings*, 2003 International Symposium on Physical Design, New York, NY, USA, 2003, pp. 10-17
[5] Yeh, R.-H., Liaw, S.-P., Tu, Y.-P., Transient Three-Dimensional Analysis of Gas Tungsten Arc Welding Plates, *Numerical Heat Transfer, Part A, 51* (2007), 6, pp. 573-592
[6] Lazić, V. N., *et al*., Determining of Cooling Time ($t_{8/5}$) in Hard Facing of Steels for Forging Dies, *Thermal Science, 14* (2010), 1, pp. 235-246
[7] Perret, W., Schwenk, C., Rethmeier, M., Comparison of Analytical and Numerical Welding Temperature Field Calculation, *Computational Materials Science, 47* (2010), 4, pp. 1005-1015
[8] Berković, M., Maksimović, S., Sedmak, A., Analysis of Welded Joints by Applying the Finite Element Method, *Integritet i Vek Konstrukcija, 4* (2004), 8, pp. 75-83

Paper submitted: September 30, 2010
Paper revised: January 3, 2011
Paper accepted: February 25, 2011